LARGE EDDY SIMULATION OF TURBULENT FLOWS IN COMPOUND CHANNELS WITH A FINITE ELEMENT CODE

C. M. Xavier, A. P. Petry and S. V. Möller
PROMEC – Programa de Pós Graduação em Engenharia Mecânica
UFRGS – Universidade Federal do Rio Grande do Sul
Porto Alegre, RS, Brazil
carla.xavier@ufrgs.br, adrianep@mecanica.ufrgs.br, svmoller@ufrgs.br

Abstract

This paper presents the numerical investigation of the developing flow in a compound channel formed by a rectangular main channel and a gap in one of the sidewalls. A three dimensional Large Eddy Simulation computational code with the classic Smagorinsky model is introduced, where the transient flow is modeled through the conservation equations of mass and momentum of a quasi-incompressible, isothermal continuous medium. Finite Element Method, Taylor-Galerkin scheme and linear hexahedrical elements are applied. Numerical results of velocity profile show the development of a shear layer in agreement with experimental results obtained with Pitot tube and hot wires.

Keywords: Turbulent Flow, Compound Channels, Finite Elements, Subgrid Scale Models, Hot wires.

1. Introduction

Compound channels are found in several branches of the engineering, from rod bundles of nuclear reactors and heat exchangers to irrigation channels with flood plains in hydraulical engineering, or finned channels for cooling of electronic devices. Basically, the cross section of a compound channel is formed by a narrow region (gap) connected to a wider one, or, conversely, a narrow region connecting two wider regions. In nuclear reactors, the narrow gap between the rods connects parallel subchannels. The investigation of the turbulent flow in this channel type show peculiar characteristics in relation to stress distribution and the coefficient of turbulent heat transfer location on the region between two channels.

Experimental measurements in a single line rod bundle showed high values of turbulence intensity for the axial and azimuthal components of velocity in the region of the gap and a strong relationship between the increase in these quantities and decreasing the distance between the tubes [1]. Fluctuations of the different velocity components showed a quasi-periodic behavior close to gap, exactly as identified previously in [2], which suggested that these pulsations of the flow were responsible for the increase in turbulent intensities along the gap.

The velocity distribution and characteristics of the turbulent flow in channels with rectangular gap in the sidewall at a range of Reynolds numbers from 2300 to 100000 was investigated experimentally in [3]. Flow visualizations showed consistent, stable and equally spaced structures transported by the mean flow inside the gap.

The characteristics of the turbulent flow in two channels connected by a rectangular gap, near the upper wall, using large eddy simulation with periodic boundary conditions in the main flow direction was presented in [4]. The height and width of the channel were respectively 180 mm and 331.6 mm with a length of 504 mm. The gap that connects the two main channels has height d and width g of 10.20 mm and 40.6 mm respectively, being the ratio g/d = 4. The Reynolds number of the simulation ranged from 3300 to 580000. The results showed peak Reynolds stresses along the gap and large vortices carried by the mean flow rotating in opposite directions, as modeled in [1].

In [5], a detailed LES study to capture the pulsating flow in compound channels in a rectangular duct forming two wide regions connected by a gap is presented.

In his Thesis, Goulart [6], established the relation between the distribution of velocity and velocity fluctuations and the mixing layer theory and proposed a Strouhal number definition to describe the dimensionless frequency of the pulsations

Recently, Meyer [7] made a comprehensive review of the flow pulsations in rod bundles, including the knowledge obtained in several types of compound channels. He concludes that the origin of this phenomenon is still disputed and that there is an analogy between flow pulsations and the mixing layer formed by two flows with different velocities merging from a split plate.

The purpose of this paper is to present a numerical code for the study of the developing turbulent flow in compound channels. The code employs the finite element method to perform large eddy simulation of the transient, quasi-incompressible, three-dimensional channel flow [8], using the Smagorinski model [9], with eight node hexahedrical elements solved by an explicit Taylor-Galerkin scheme. The geometry of the channel consists on a main channel connected to a gap on a side wall. Results are compared with experimental results obtained with Pitot tube and hot wires in an aerodynamic channel.

2. Test Section and Computational Domain

The investigations were made in a rectangular channel with 146 mm height and 193 mm in width, where in a side wall is a gap where the flow develops. The gap was 2000 mm long with a depth d = 80 mm and width g = 20 mm, thus having a d/g-ratio equal to 4. The working fluid used is air at room temperature, driven by a centrifugal blower passing through a diffuser, a homogenizer and two screens, reaching the test section with turbulence intensity less than 1%. At 150 mm downstream of the screens a Pitot tube is located, to measure the reference velocity U_{REF}, which is approximately equal to the mean velocity in the channel. The Reynolds numbers of experiment and simulation were calculated using the mean velocity of the flow in the test section and its hydraulic-diameter, D_h = 131.08 mm, ranging from Re = 100 to Re = 85,000. Figure 1 (a) shows a schematic view of the test section studied, where the red line shows the location of the gap while Fig. 1 (b) and (c) shows schemes of the cross section with location of hot wire measurements.

The average values of the axial velocity component were measured using a Pitot tube with outside diameter of 1.25 mm. While the velocity fluctuations in x and z directions were obtained via hot wire anemometry, using a constant temperature probe DANTEC StreamLine. The axial velocity component, u, is parallel to main flow direction and the transverse component, w, is parallel to the symmetry line. In the simultaneous measurement of two velocity components a double wire probe was used, which has a wire perpendicular to the main flow and a slant (45°) wire. Probe calibration and evaluation of velocities were made using Collis and Williams method [10, 11].

The Pitot tube and hot wire probe were moved along the symmetry line of the channel by means of a tri-axial positioner. Data acquisition of hot wire signals was done using a 16 bit analog digital converter board (National Instruments 9215-A), and a sampling frequency of 3KHz. The length of the records was 21.84 s. The average error in determining the velocity with the hot wire anemometer was approximately 3%.

In the computational domain, the channel is represented by a uniform mesh composed by 98,112 nodes. The mesh is shown in Figure 2 and represents accurately the test section.

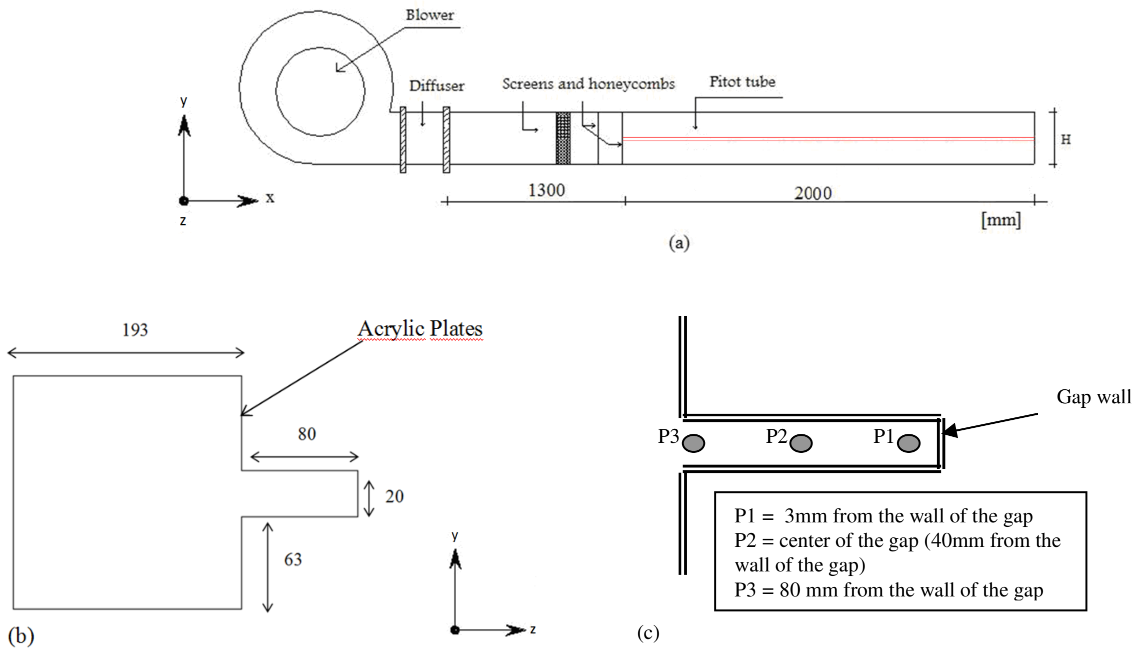

Figure 1 Schematic view of the test section: a) side view of the channel, b) cross section of the channel, c) location of hot wire measurements.

3. Mathematical and Numerical Aspects

3.1. Governing equations

In large eddy simulations, balance equations for mass, energy and momentum of a viscous, quasi-incompressible, three-dimensional, transient and isothermal flow of a newtonian fluid [12; 13; 8] are decomposed into large-scale field (identified by the bar over the variable) and subgrid scale field (identified by the apostrophe). Filtered velocity and pressure are

$$v_i = \overline{v_i} + v_i' \qquad p = \overline{p} + p' \qquad (1)$$

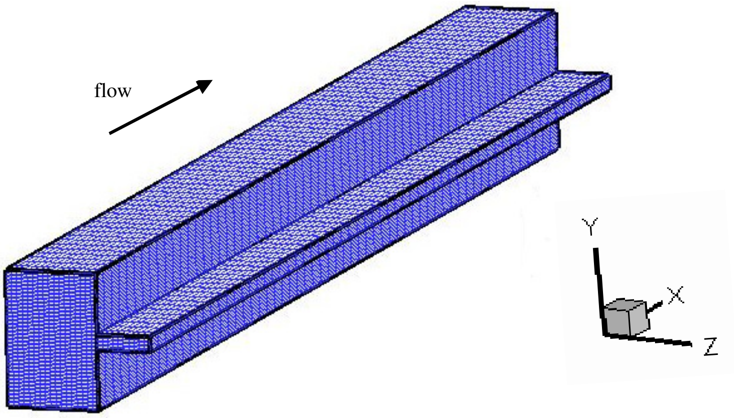

Figure 2 3D-scheme of channel geometry and Computational grid

Filtered equations of mass and momentum are given by:

$$\frac{\partial \overline{p}}{\partial t} + C^2 \frac{\partial}{\partial x_j}\left(\rho \overline{v}_j\right) = 0 \tag{2}$$

$$\frac{\partial}{\partial t}(\rho \overline{v}_i) + \frac{\partial}{\partial x_j}\left(\rho \overline{v}_i \overline{v}_j\right) + \frac{\partial \overline{p}}{\partial x_j}\delta_{ij} - \frac{\partial}{\partial x_j}\left\{ \nu\left(\frac{\partial}{\partial x_j}(\rho \overline{v}_i) + \frac{\partial}{\partial x_i}(\rho \overline{v}_j)\right) + \frac{\lambda}{\rho}\left(\frac{\partial}{\partial x_k}(\rho \overline{v}_k)\right)\delta_{ij}\right\}$$
$$+ \frac{\partial}{\partial x_j}\left\{\rho\left(L_{ij} + C_{ij} + \overline{v'_i v'_j}\right)\right\} - f_i = 0$$

$$(j = 1, 2, 3) \ in \ \Omega \tag{3}$$

With boundary conditions:

$$v_i = \hat{v}_i \qquad in \ \Gamma_v \tag{4}$$

$$\left\{\left[-\overline{p} + \frac{\lambda}{\rho}\frac{\partial}{\partial x_k}\left(\rho \overline{v_k}\right)\right]\delta_{ij} + \nu\left[\frac{\partial}{\partial x_j}\left(\rho \overline{v_i}\right) + \frac{\partial}{\partial x_i}\left(\rho \overline{v_j}\right)\right]\right\} n_j = t_i \qquad in \ \Gamma_t \tag{5}$$

and the corresponding initial conditions:

$$v_i = \hat{v}_{i0} \qquad in \ t = 0, \Omega \tag{6}$$

$$p = \hat{p}_0 \qquad in \ t = 0, \Omega \tag{7}$$

Where:
$\rho \rightarrow$ fluid density (kg/m^3)
$v_i \rightarrow$ velocity component in direction i (m/s)
$x_i \rightarrow$ coordinate in i direction (m)

$\delta_{ij} \rightarrow$ Kronecker delta

$\hat{v}_i \rightarrow$ velocity i values prescribed on the boundary indicated (m/s)

$n_j \rightarrow$director cosine of the vector normal to the boundary

$t_i \rightarrow$ prescribed values of surface forces on the boundary (N)

$\mu \rightarrow$ Coefficient of dynamic viscosity of the fluid (Pa.s)

$\lambda \rightarrow$ Coefficient of viscosity of the fluid volume (Pa.s)

$C \rightarrow$ velocity of sound propagation (m/s)

$\nu \rightarrow$ kinematic viscosity (m^2/s)

$\overline{v}_i \rightarrow$ component, corresponding to large scales, the velocity vector in the direction xi (m/s).

$\overline{p} \rightarrow$ pressure component corresponding to large scales (Pa).

$v'_i \rightarrow$ velocity component in the direction x_i, corresponding to the subgrid scales (m/s)

$L_{ij} = \overline{\overline{v}_i \overline{v}_j} - \overline{v}_i \overline{v}_j \rightarrow$ terms of Leonard.

$C_{ij} = \overline{\overline{v}_i v_j'} + \overline{v_i' \overline{v}_j} \rightarrow$ cross terms.

$\overline{v_i' v_j'} \rightarrow$ Reynolds tensor subgrid scale (m^2/s^2).

$\Omega \rightarrow$ problem domain

$\Gamma_v \rightarrow$face boundary with prescribed velocity

$\Gamma_t \rightarrow$face with natural boundary condition

Leonard and cross terms L_{ij} and C_{ij} can be neglected [13]. Previous studies, in [8], confirms that the inclusion of these terms do not significantly affect the results and increase around 20% processing time. Therefore, neglecting Leonard's and cross terms, equations (2) and (3), with the initial and boundary conditions given by Equations (4), (5), (6) and (7) are the governing equations. For the solution of the system a subgrid scale model must be used. The quasi incompressible analysis assumes a constant density throughout the flow domain, but the sound velocity is not considered infinite. As a result of this consideration, time derivative of the pressure appears in mass conservation equation (Eq. 2), simplifying the handling of the equation system [8].

3.2. Subgrid Scale Models

The model is implemented based on the concept of turbulent viscosity and using the Boussinesq hypothesis, the Reynolds stress subgrid scales are given by:

$$-\overline{v_i' v_j'} = \nu_t \left(\frac{\partial \overline{v}_i}{\partial x_j} + \frac{\partial \overline{v}_j}{\partial x_i} \right) \tag{8}$$

where ν_t is the turbulent viscosity.

For incompressible flows, this equation is usually modified by introducing a subgrid scale kinetic energy term to make the model compatible with the mass conservation equation for incompressible flows [14]. But in this work, the equation of continuity is modified for quasi-incompressible flows, maintaining, therefore, Equation (8) in its original form.

The Smagorinsky model [9] has been traditionally used to represent the effect of the subgrid scales in large eddy simulation [13, 15], being a turbulent viscosity model in which the Reynolds stresses are given by a subgrid scale, Equation (8), and the turbulent viscosity is defined as:

$$\nu_t = C_S^{\,2}\,\overline{\Delta}^2\left|\overline{S}\right| \tag{9}$$

Where C_S is the Smagorinsky constant and other terms are given by:

$$\left|\overline{S}\right| = \sqrt{2\overline{S}_{ij}\overline{S}_{ij}} \tag{10}$$

$$\overline{S}_{ij} = \frac{1}{2}\left(\frac{\partial \overline{v}_i}{\partial x_j} + \frac{\partial \overline{v}_j}{\partial x_i}\right) \tag{11}$$

$$\overline{\Delta} = \sqrt[3]{\prod_{i=1}^{3}\Delta x_i} \tag{12}$$

For the solution of the system of equations, the Finite Element Method is employed. To get the system of algebraic equations, time derivatives are expanded in Taylor series, including the second order terms, and for the space discretization the classic Galerkin method is applied [17]. To save processing time, analytical expressions for the elements matrices are used for the hexaedrical isoparametric element [18]. This scheme is known as Taylor-Galerkin, [19. The scheme is explicit and conditionally stable and the integration time step has the following restriction:

$$\Delta t \le \frac{\Delta x_i(\min)}{C+V} \tag{13}$$

where Δx_i (min) is the minimum dimension of the mesh elements, C is the speed of sound and V is the reference velocity (V_{ref}). Details of the numerical methodology can be found in [8].

As boundary conditions at the entrance, a turbulent velocity profile was adopted (v1 = V (y), v2 = 0, v3 = 0) and non-slip condition (v1 = v2 = v3 = 0) for all walls. For the outlet, natural boundary conditions (t1 = t2 = t3 = 0) were prescribed (see Equation (5)). The initial conditions used are v1 = V_{ref} (steady value), v2 = v3 = p = 0.

3.3 Numerical Simulation

Large eddy simulations of the three-dimensional flow in the compound channel investigated were performed successively with Reynolds number Re=100, 3300 and 10000. When a simulation is completed, the resulting velocity field is used as initial condition for the next simulation with a higher Reynolds number to reduce the computation time for the higher Reynolds numbers. Therefore, the results presented in this paper will be used for computation with Re = 50000 and then to Re = 85000 (experimental).

The code uses a parallel processing OpenMP architecture, which allows the solution of large and complex problems, like the compound channel discussed in this work, with the same code, only by the distribution of computational load, taking advantage of all available resources. The language of the code is FORTRAN 95, using high performance techniques. To ensure its portability and facilitate modifications, the code has a modular structure (each module is a set of subroutines stored in a different file), allowing a selective compilation by adding or deleting routines. Dimensionless mesh size has values of $\Delta x^+ = 27.73$; $\Delta y^+ = 2.31$ and $\Delta z^+ = 7.39$, defined with the mesh size in x, y and z directions, the friction velocity in the domain entry and the kinematic viscosity. The time step used for Re = 100 was 5.10^{-4} s, while for Re = 3300 and Re = 10000 it was 1.10^{-5} s, the Smagorinsky constant, C_s, was 0.23. The convergence criteria adopted was 1.10^{-4}.

4. Results

Figure 3-a show the axial velocity contours obtained with a Pitot tube in the gap region of the channel, 50mm before outlet. The results are presented together with velocity values obtained from the simulation results for Re = 10000. It is observed a region of maximum velocity occurring in the main channel and a level of nearly constant velocity in the gap region. The excessive deflection of isovelocity lines indicates the influence of the secondary flows; in accordance with experimental results in [3] and recent simulations [16].

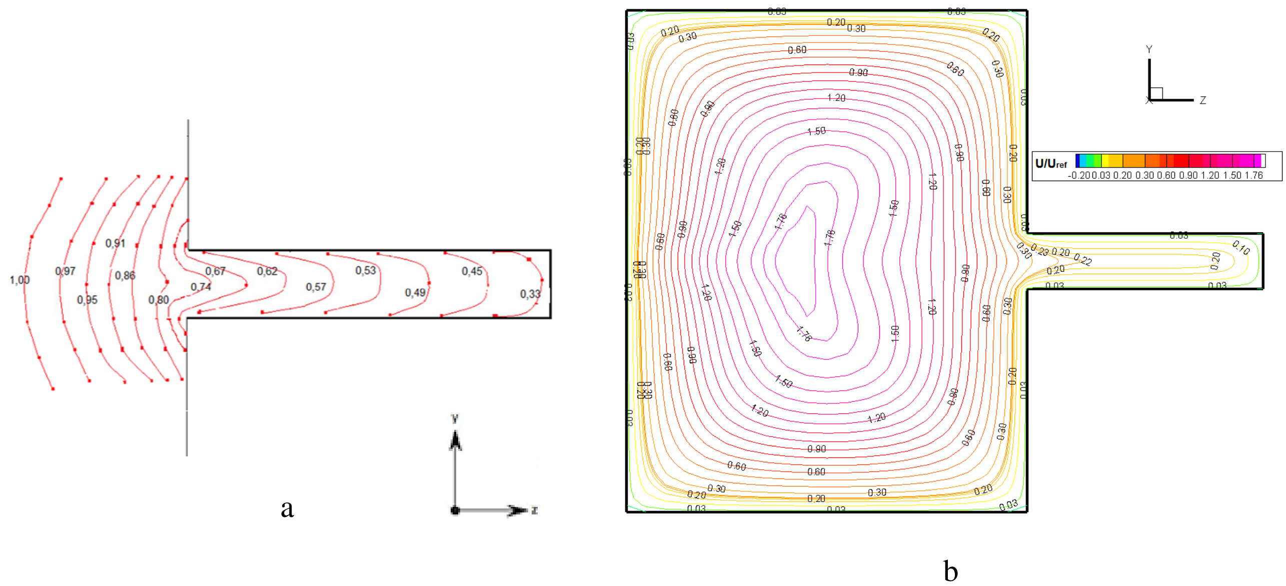

Figure 3 Contours of axial mean velocity, 50 mm upstream of the channel outlet (x/L = 0.98) a) Re = 85000 - experimental; b) Re = 10000 – numerical.

The presence of coherent structures is firstly observed by the presence of peaks in spectra of axial and transversal velocity fluctuations (toward the gap). By using the Strouhal number definition proposed in Ref. [3], given by

$$Str = \frac{f}{U_c}\sqrt{g.d} \qquad (14)$$

with Str=0.066, the frequency obtained for the Reynolds number investigated is f=16.5 Hz. Figure 4 shows maximal values of the spectra at 25Hz, higher than the calculated value, but still in the same order of magnitude. The linear dependence of the frequency on the flow velocity [1, 3] allows the comparison of frequencies to be obtained in the numerical simulation.

Figure 5-a shows the axial mean velocity profiles measured along the symmetry line in the outlet of the channel as a function of the position in z coordinate. The value z/d =1, corresponds to the edge of the gap. There, one can see the velocity profile divided up into three different zones: while in external zones velocity distribution is influenced by the walls on the extremities of the symmetry line, in the central zone, the flow has characteristics of a mixing layer beginning in the region between the plates and extending towards the main channel. In spite of the difference in the Reynolds number, the code underestimates the flow velocity in the gap region. This is attributed to the coarse grid employed in this calculation. Maximum in the velocity gradients, Fig. 4-b, shows the location of the inflection point of the velocity profile. The width of the central zone is the mixing layer thickness δ in [6].

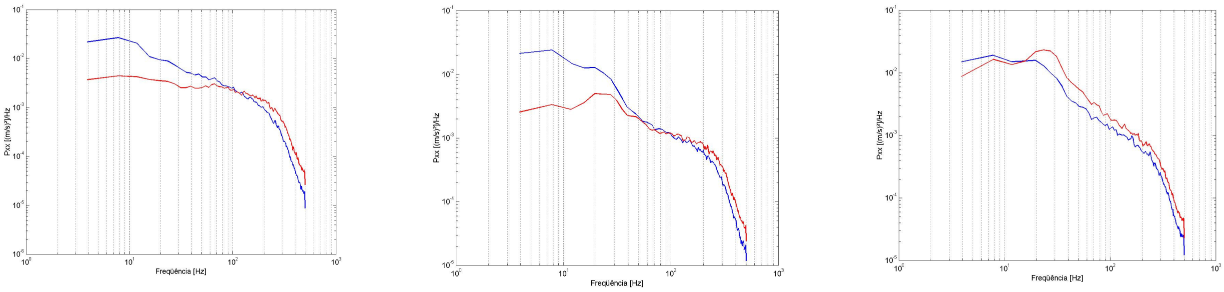

a b c

Figure 4 Autospectral density of axial (blue) and transversal (red) velocity fluctuation: a) P1; b) P2; c) P3. Locations given in Fig. 1-c.

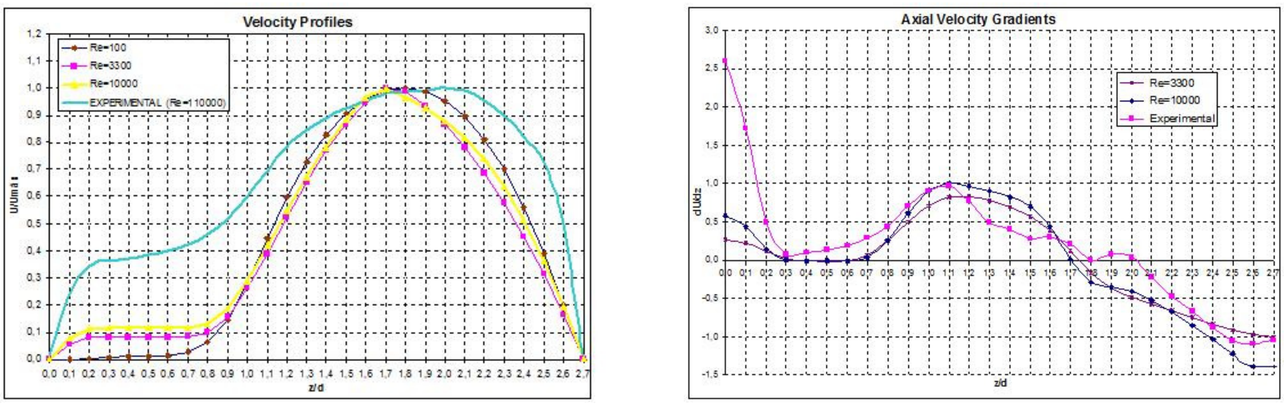

a b

Figure 5 a) Axial velocity profiles; b) Axial velocity gradients.

In Figure 6, the flow development can be observed through the axial velocity distribution in the symmetry plane of the test section. The reduction of the flow velocity in the gap region is accompanied by its increase in the main channel. The mass transport from the gap to the main channel can be observed by the deflection of the isovelocity lines in Fig. 3-b. Since the flow is not fully developed at the outlet, the shear layer in the gap region may not produce defined pulsations as observed in [3] for the same geometry. This can be the reason for the discrepancy in the calculated frequency through the correlation for Strouhal number given in [3] and the experimental frequency. This can also be observed in the isovorticity map in the same plane, Fig. 7. The vorticity in the XZ plane is given by:

$$\Omega_y = \frac{1}{2}\left[\left(\frac{\partial u}{\partial z}\right) - \left(\frac{\partial w}{\partial x}\right)\right] \tag{15}$$

Isovorticity values are very high as expected near the walls. In the extremity of the gap, lines show the presence of a wake like structure, in the region of corresponding to z/d=0.8 to 1.7 (in Figure 5).

For Figs. 6 and 7, the mesh was refined in the gap region with values $\Delta x^+ = 1.15$, $\Delta y^+ = 0.05$ and $\Delta z^+ = 0.174$.

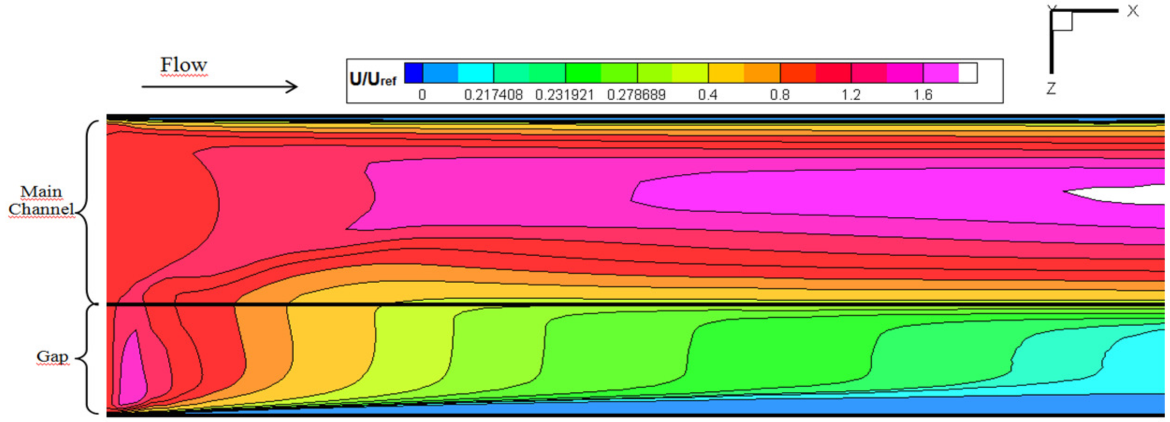

Figure 6 Axial velocity distribution in the plane of the gap (numerical: Re = 10000).

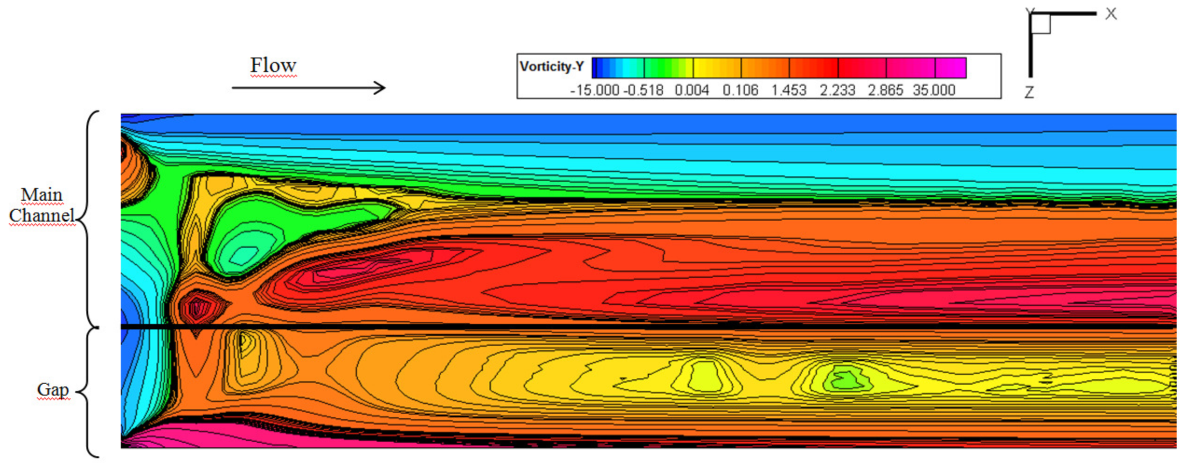

Figure 7 Isovorticity Ω_y distribution in the plane of the gap (numerical: Re = 10000).

In Fig. 8 a and b, the RMS values of axial and transversal velocity fluctuations along the symmetry line are shown as a function of the position z/d. In the region of the highest vorticity values, an increase in the axial and transversal turbulence intensity is observed, confirming the formation of turbulent structures corresponding to the presence of pulsations in the flow. The location of the maxima is outside the gap, as a result of the underestimation of the velocity inside the gap due to the coarse grid adopted.

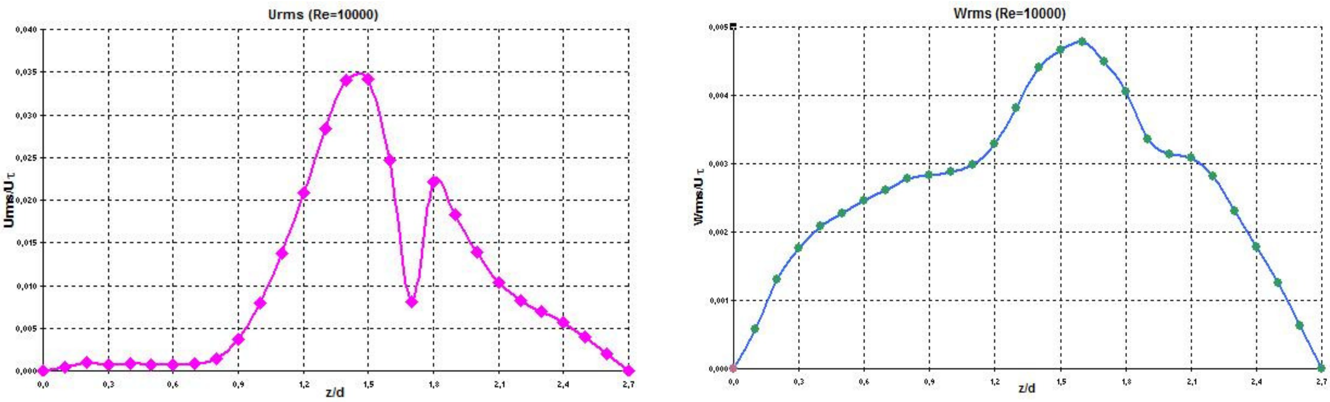

a b

Figure 8 RMS values of:
a) Axial velocity fluctuations; b) Transversal velocity fluctuations.

6. Conclusions

This paper presents a finite element computer code for solving the turbulent flow in a compound channel formed by a rectangular cross section region connected to a slot. The numerical methodology is the large eddy simulation with a Smagorinsky model. The turbulent flow is considered quasi-incompressible, isothermal and transient.

The results are consistent with the experimental data. Discrepancies in the calculated frequency for the pulsation using the correlation for the Strouhal number given in [3] and the experimental frequency obtained is attributed to the flow development process not completed at the test section outlet. The coarse grid adopted allowed the fast debugging of the code but the velocity in the gap was underestimated. The increase of the Reynolds number to 50000 and to 85000 will allow direct comparison with the experimental results.

The use of the numerical code applied to the studied problem has shown the ability of this methodology to simulate complex turbulent flows, without limitations on memory allocation. However, the very short integration time step leads to long processing times as the Reynolds number increases. The use of a more refined mesh, now in progress, will bring improvements in flow analysis mainly in the region of the gap.

7. Acknowledgements

Authors gratefully acknowledge the support by The National Council for Scientific and Technological Development (CNPq), Ministry of Science and Technology (MCT), Brazil.

Authors thank also the National Center for Supercomputing - Southern Region, Federal University of Rio Grande do Sul (CESUP-RS/UFRGS).

Carla M. Xavier is also grateful to CAPES- Ministry of Education, Brazil, for granting her a fellowship.

8. References

[1] S. V. Möller, 1991, "On Phenomena of Turbulent Flow through Rod Bundles". Experimental Thermal and Fluid Science, v. 4, n.1, pp. 25-35.

[2] D. S. Rowe, B. M. Johnson and J. G. Knudsen, 1974, "Implications concerning rod bundle cross flow mixing based on measurements of turbulent flow structure", Int. J. Heat Mass Transfer, 17, 407-419.

[3] L. Meyer and K. Rehme, 1995, "Periodic vortices in flow though channels with longitudinal gaps or fins", 10th Symposium on turbulent shear flows, The Pennsylvania State University, University Park, August 14-16.

[4] M. Biemüler, L. Meyer, and K. Rehme, 1996, "Large eddy simulation and measurement of the structure of turbulence in two rectangular channels connected by the gap", Engineering Turbulence Modeling and Experiments 3, Editors: W. Rodi and G. Bergeles, 249-258.

[5] E. Merzari, H. Ninokata, E. Baglietto, 2008, "Numerical simulation of flows in tight-lattice fuel bundles". Nucl. Eng. Des. 238, 1703–1719.J.

[6] J. N. V. Goulart, 2009, " Experimental Study of the Turbulent Shear Flow in Closed Compound Channels" (in Portuguese), Dr. Thesis, PROMEC, Federal University of Rio Grande do Sul, Brazil. Available on line at http://hdl.handle.net/10183/16204.

[7] L. Meyer, 2010, "From discovery to recognition of periodic large scale vortices in rod bundles as source of natural mixing between sub-channels - A review", Nuclear Engineering and Design, Vol.240, Issue 6, Pages 1575-1588.

[8] A. P. Petry, A. M. Awruch, 2006, " Large Eddy Simulation of Three-Dimensional Turbulent Flows by the Finite Element Method" . Journal of the Brazilian Society of Mechanical Sciences and Engineering, Vol. XXVIII, pp. 224-232.

[9] J. Smagorinsky, 1963, "General circulation experiments with the primitive equations. I. The basic experiment", Monthly Weather Reviews, v. 91, pp. 99-164.

[10] D. C. Collins, M. J. Williams, 1959, "Two-dimensional convection from heated wires at low Reynolds numbers". Journal of Fluid Mechanics, v. 6, pp. 357-384.

[11] C. R. Olinto and S. V. Möller, 2004, "X-probe calibration using Collis and William's equation". In: 10th Brazilian Congress of Thermal Sciences and Engineering – ENCIT 2004, Rio de Janeiro, Brazil.

[12] M. Kawahara, H. Hirano, 1983. "A Finite Element Method for High Reynolds Number Viscous Fluid Flow Using Two Step Explicit Scheme". International Journal for Numerical Methods in Fluids, V.3, pp.137-163.

[13] A. N. Findikakis and R. L. Street, 1982, "Mathematical Description of Turbulent Flows", Journal of Hydraulics Division, ASCE, V108, N°.HY8, paper 17265, p887-903.

[14] O. Hinze, 1975. "Turbulence", McGraw-Hill, New York.

[15] M. Lesieur, P. Comte, O. Métais, 1995, "Numerical simulations of coherent vortices in turbulence", ASME - Appl Mech Rev, Vol. 48, N°.4.

[16] D. Home, G. Arvantinis, M. F. Lightstone and M. S. Hamed, 2009, " Simulation of flow pulsations in a twin rectangular sub-channel geometry using unsteady Reynolds Averaged Navier-Stokes modeling", Nuclear Engineering and Design, 239, pp. 2964-2980.

[17] Reddy, J.N., Gartling, D.K.. 1994, The Finite Element Method in Heat Transfer and Fluid Dynamics, CRC Press.

[18] Burbridge, H.P., Awruch, A.M., 2000, An efficient one-step Taylor-Galerkin Scheme to Analyze 3D High Compressible Flows Using the Finite Element Method, In: 8th Brazilian Congress of Thermal Sciences and Engineering - ENCIT 2000, Porto Alegre, RS, Brasil.

[19] Donea, J, 1984, "A Taylor-Galerkin Method for Convective Transport Problems", International Journal for Numerical Methods in Engineering, Vol.20, pp. 101-119.